

Originally published as:

Förster, H.-J., Bindi, L., Stanley, C. J., Grundmann, G. (2017 online): Hansblockite, (Cu,Hg)(Bi,Pb)Se2, the monoclinic polymorph of grundmannite: a new mineral from the Se mineralization at El Dragón (Bolivia). - *Mineralogical Magazine*, *81*, 3, pp. 629—640.

DOI: http://doi.org/10.1180/minmag.2016.080.115

- 1 Hansblockite, (Cu,Hg)(Bi,Pb)Se<sub>2</sub>, the monoclinic polymorph of
- 2 grundmannite: a new mineral from the Se mineralization at El Dragón
- 3 (Bolivia)
- 4 HANS-JÜRGEN FÖRSTER<sup>1,\*</sup>, LUCA BINDI<sup>2</sup>, CHRIS J. STANLEY<sup>3</sup> AND GÜNTER GRUNDMANN<sup>4</sup>
- <sup>1</sup> Helmholtz Centre Potsdam German Research Centre for Geosciences GFZ,
- 6 D-14473 Potsdam, Germany
- 7 \*E-mail: hans-juergen.foerster@gfz-potsdam.de
- 8 <sup>2</sup> Dipartimento di Scienze della Terra, Università degli Studi di Firenze, Via G. La Pira 4,
- 9 I-50121 Firenze, Italy

- 10 <sup>3</sup> Department of Earth Sciences, Natural History Museum, Cromwell Road,
- 11 London SW7 5BD, United Kingdom
- 12 <sup>4</sup> Eschenweg 6, D-32760 Detmold, Germany
- 14 **ABSTRACT:** Hansblockite, ideally (Cu,Hg)(Bi,Pb)Se<sub>2</sub>, is a new selenide from the El Dragón
- mine, Bolivia. It typically occurs in thin plates subparallel intergrown with two unnamed
- 16 Cu-Hg-Pb-Bi-Se species, clausthalite, Co-rich penroseite, and petrovicite. It also forms sub-
- to anhedral grains up to 150 μm in length and 50 μm in width. Hansblockite is non-
- 18 fluorescent, black and opaque with a metallic luster and black streak. It is brittle, with an
- irregular fracture and no obvious parting and cleavage. The VHN<sub>20</sub> values range from 37 to 50
- 20 (mean 42) kg mm $^{-2}$  (Mohs hardness  $2-2\frac{1}{2}$ ). In plane-polarized incident light, hansblockite is
- 21 cream to light grey in colour, weakly bireflectant and weakly pleochroic from greyish cream
  - to cream. Under crossed polars, hansblockite is weakly anisotropic with khaki to pale blue

- rotation tints. The reflectance values in air for the COM standard wavelengths are: 47.3–48.1
- 24 (470 nm), 47.4–49.9 (546 nm), 47.1–49.0 (589 nm), and 46.6–48.5 (650 nm). The mean
- 25 composition is Cu 9.31, Ag 0.73, Hg 11.43, Pb 3.55, Ni 0.17, Co 0.03, Bi 31.17, Se 34.00,
- total 100.39 wt.%. The mean empirical formula (based on 4 atoms *pfu*) is
- 27  $(Cu_{0.68}Hg_{0.27}Ag_{0.03}Ni_{0.01})_{\Sigma=0.99}(Bi_{0.69}Pb_{0.31})_{\Sigma=1.00}Se_{2.01}$ . The simplified formula is
- (Cu,Hg)(Bi,Pb)Se<sub>2</sub>. Hansblockite is monoclinic, space group  $P2_1/c$ , with a 6.853(1) Å, b
- 29 7.635(1) Å, c 7.264(1) Å, β 97.68(1)°, V 376.66(9) Å<sup>3</sup>, and Z = 4. Density is 8.26 g cm<sup>-3</sup>.
- The five strongest X-ray powder-diffraction lines  $[d \text{ in } Å(I/I_0) (hkl)]$  are: 3.97 (90) (111),
- 3.100 (40) (-121), 2.986 (100) (-211), 2.808 (50) (112), and 2.620 (50) (022). Hansblockite
- represents the monoclinic polymorph of grundmannite, CuBiSe<sub>2</sub>, with Hg and Pb being
- essential in stabilizing the monoclinic structure via the coupled substitution  $Cu^+ + Bi^{3+} \Leftrightarrow$
- $Hg^{2+} + Pb^{2+}$ . The mineral name is in honour of Hans Block (1881–1953), in recognition of his
- important role in boosting Bolivian ore mining.
- 37 **Keywords**: hansblockite; new mineral species; chemical composition, crystal structure;
- 38 selenium; El Dragón, Bolivia

#### Introduction

36

39

- 41 The Andes of Bolivia host two volumetrically minor, but mineralogically important selenide
- occurrences: Pacajake, district of Hiaco de Charcas, and El Dragón, Province of Antonio
- 43 Quijarro, both in the Department of Potosí. The geology and ore mineralization of the El
- Dragón mine was first explored in detail by Grundmann *et al.* (1990). Recently, it received
- renewed attention as the type locality of eldragónite, Cu<sub>6</sub>BiSe<sub>4</sub>(Se<sub>2</sub>) (Paar *et al.*, 2012), and
- 46 grundmannite, CuBiSe<sub>2</sub> (Förster et al., 2016), and the discovery of the two new Se-bearing

47 secondary species favreauite, PbBiCu<sub>6</sub>O<sub>4</sub>(SeO<sub>3</sub>)<sub>4</sub>(OH) · H<sub>2</sub>O (Mills et al., 2014), and alfredopetrovite, Al<sub>2</sub>(Se<sup>4+</sup>O<sub>3</sub>)<sub>3</sub>· 6H<sub>2</sub>O (Kampf *et al.*, 2016). 48 49 In addition to the recently described Cu–Bi sulfosalts eldragónite and grundmannite, 50 three unnamed species of the Cu-Hg-Pb-Bi-Se system have been discovered in samples from the El Dragón mine, labelled phases "A", "B", and "C" (cf. Paar et al., 2012; Förster et 51 52 al., 2016). The new selenium mineral, hansblockite (Cu,Hg)(Bi,Pb)Se<sub>2</sub>, described in this paper resembles phase "B", for which initially the ideal formula Cu<sub>2</sub>HgPbBi<sub>2</sub>Se<sub>6</sub> (normalized 53 54 to 12 apfu) was proposed (Paar et al., 2012; Förster et al., 2016). 55 The new species hansblockite and its name have been approved by the Commission on 56 New Minerals, Nomenclature and Classification (CNMNC) of the IMA, proposal 2015–103. The holotype specimen, which is the polished section from which the grain used for crystal-57 structure determination was obtained, is stored in the collections of the Natural History 58 Museum, London, catalogue number BM 2015, 136. Cotype material, consisting of a 59 hansblockite-bearing section, is deposited within the Mineralogical State Collection Munich 60 61 (Mineralogische Staatssammlung München, Museum "Reich der Kristalle"), inventory 62 number MSM 73573. The name is in honour of Hans Block (1881–1953), in recognition of his contribution 63 to fostering Bolivian ore mining. Born in Stassfurt, Alemania, Germany, he emigrated to 64 65 Bolivia in 1904, when he was contracted by the Compania Huanchaca de Bolivia, the plant operator for the Pulacayo mine. He was later administrator, manager, and owner of several 66 67 mines, among them the Compania Minera Gallofa Consolidada de Colquechaca (e.g., Block, 68 1937; Block and Ahlfeld, 1937). In 1945, Hans Block became a Professor of the Facultad 69 Nacional de Ingenieria in Oruro. In 1952, he was appointed to the Commission for the

70

Nationalization of the Mines.

It is important to note that Herzenberg and Ahlfeld (1935) named a mineral from the
lead-silver mine Hiaco, Colquechaca, Bolivia in honour of Hans Block "blockite". Later,
Bannister and Hey (1937) demonstrated that "blockite" was identical to penroseite and
concluded that the mineral name "blockite" should be discarded. To avoid confusion with two
different blockite names in the literature, the name hansblockite was proposed for the present
new selenide.

## **Geological setting**

The El Dragón selenide occurrence is situated in southwestern Bolivia, in the Cordillera Oriental, some 30 km southwest of Cerro Rico de Potosí. The abandoned El Dragón mine (entrance and dump) is located 19° 49' 23.90" S (latitude), 65° 55' 00.60" W (longitude), at an altitude of 4160 m above sea level. The very small longitudinal extension (maximum 15-m-long gallery) of the El Dragón ore vein and its low silver content (averaging to 0.06 wt.% Ag) have probably discouraged further exploitation of the occurrence.

The adit of the El Dragón mine is on the orographic left side of the Rio Jaya Mayu, cutting through a series of thinly-stratified, pyrite-rich black shales and reddish-grey, hematite-bearing siltstones of probably Devonian age, dipping 40° to the north. The almost vertical ore vein is located in the center of a 1.5-m-wide shear zone (average trend 135 degrees) with shifts of a few cm. In 1988, the selenium mineralization consisted of a single vein, ranging mostly from 0.5 to 2 cm in thickness.

The El Dragón mineralization is composed of a complex assemblage of primary and secondary minerals, among which Se-bearing phases are most prominent. The full list of minerals recorded from El Dragón is given on mindat.org at <a href="http://www.mindat.org/loc-353.html">http://www.mindat.org/loc-353.html</a>. Grundmann *et al.* (1990) and Paar *et al.* (2012) provided detailed descriptions of the entire mineralization.

98

99

102

103

104

105

106

107

108

109

110

111

114

115

117

119

120

## Appearance and physical properties

Hansblockite typically occurs in lath-shaped thin plates (up to 100 µm in length and 10 µm in width) intimately (subparallel) intergrown with unnamed phase "A" (empirical formula 100 Cu<sub>5</sub>HgPb<sub>2</sub>Bi<sub>3</sub>Se<sub>10</sub>; Paar et al., 2012) and, less frequently, with unnamed phase "C" (empirical formula Cu<sub>4</sub>HgBi<sub>4</sub>Pb<sub>2</sub>Se<sub>11</sub>; Förster et al., 2016, their Figure 2d–e), forming an angular 101 network of tabular hansblockite crystals (Fig. 1). Among these species of the Cu-Hg-Pb-Bi-Se system forming these multi-phase aggregates, phase "A" generally appears to have crystallized earliest in the cores, partially overgrown by hansblockite predominantly forming the rims (Fig. 1). The relatively rare and small grains of phase "C" (max. 20 x 20 µm) are the relatively youngest, precipitated in the interstices between the unoriented hansblockite/phase "A" laths, together with Co-rich penroseite (NiSe<sub>2</sub>), umangite (Cu<sub>2</sub>Se<sub>3</sub>), klockmannite (CuSe), watkinsonite (ideally Cu<sub>2</sub>PbBi<sub>4</sub>Se<sub>8</sub>) and clausthalite (PbSe) (cf. Figs. 3, 4). Hansblockite-crystal aggregates cement (usually together with clausthalite, umangite, klockmannite, eldragónite and co-rich penroseite) shrinkage cracks or fill interstices in brecciated krut'aite-penroseite (CuSe<sub>2</sub>-NiSe<sub>2</sub>) solid solution. Hansblockite locally forms sub- to anhedral grains up to 200 µm in length and 50 µm 112 in width, occurring either solitary in the matrix or intergrown with watkinsonite, clausthalite, 113 eldragónite, krut'aite-penroseite solid solution, eskebornite (CuFeSe<sub>2</sub>), klockmannite and umangite (Fig. 2). Minerals occasionally being in grain-boundary contact are petrovicite 116 (Cu<sub>3</sub>HgPbBiSe<sub>5</sub>), grundmannite (CuBiSe<sub>2</sub>), and native gold. Hansblockite partially replaces umangite, klockmannite, eskebornite, and is itself altered by late klockmannite, athabascaite 118 (Cu<sub>5</sub>Se<sub>4</sub>), and late fracture-filling chalcopyrite and covellite. Secondary minerals adjacent to hansblockite encompass quartz, dolomite, calcite, goethite, lepidocrocite, chalcomenite, molybdomenite, olsacherite, schmiederite, ahlfeldite, favreauite, felsőbányaite, and allophane.

Berzelianite (Cu <sub>2-x</sub> Se) and bellidoite (Cu <sub>2</sub> Se), previously mentioned by Grundmann et a
(1990), were not detected in any sample from El Dragón.

Hansblockite was observed in  $\sim 30\%$  out of 180 microscopically studied polished sections from El Dragón, but in only 10% it occurred relatively frequently. Homogenous crystals are rare; typical are intimate intergrowths with phase "A" down to the nm-scale.

Hansblockite is non-fluorescent, black and opaque with a metallic luster and black streak. It is brittle, with an irregular fracture and no obvious parting and cleavage. The mean Vickers hardness number (VHN) for a 20 g load is  $42 \text{ kg} \cdot \text{mm}^{-2}$  (range 37-50), corresponding to a Mohs hardness of 2 to  $2\frac{1}{2}$ . Density could not be measured because of the small grain size. Density calculated on the basis of the mean chemical composition and unit-cell parameters derived from the single-crystal X-ray study is  $8.26 \text{ g} \cdot \text{cm}^{-3}$ .

### **Optical properties**

Optical properties of hansblockite are shown in Figures 3 and 4. In plane-polarized incident light, hansblockite is cream to light grey in color, slightly bireflectant and slightly pleochroic from greyish cream to cream. The mineral does not show any internal reflections. Under crossed polars, hansblockite is weakly anisotropic, with khaki to pale blue rotation tints. Under crossed polars, the differences in color are blurred. To visualize the microstructural properties more impressively, respective microphotographs 3 and 4 were taken under partly crossed polars.

Quantitative reflectance data for hansblockite were obtained in air relative to a Zeiss WTiC standard using a J and M TIDAS diode array spectrometer attached to a Zeiss Axiotron microscope. Measurements were made on unoriented grains at extinction positions leading to

designation of $R_1$ (minimum) and $R_2$ (maximum). The results are listed in Table 1 (togeth	er
with the calculated color values) and illustrated graphically in Figure 5.	

### **Chemical Composition**

All primary minerals from El Dragón were routinely analyzed for concentrations of Cu, Ag, Pb, Hg, Fe, Co, Ni, As, Sb, Bi, S and Se. Quantitative chemical analyses were conducted in WDS mode, using a JEOL thermal field-emission-type electron probe X-ray microanalyzer (FE-EPMA) JXA-8500F (HYPERPROBE) at Deutsches GeoForschungsZentrum GFZ, Potsdam, Germany. The probe was operated at 20 kV, 20 nA; the beam size was 1-2  $\mu$ m. The counting time on peak was 20-40 s, with half that time on background on both sites of the peak. The following standards, emission lines and analyzing crystals (in parentheses) were used: Cu – synthetic Cu-metal,  $K\alpha$  (LIF); Ag – naumannite,  $L\alpha$  (PETJ); Pb – clausthalite,  $M\alpha$  (PETH); Hg – cinnabar,  $L\alpha$  (LIF); Fe – pyrite,  $K\alpha$  (LIF); Co – skutterudite,  $K\alpha$  (LIF); Ni – pentlandite,  $K\alpha$  (LIF); As – skutterudite,  $L\alpha$  (TAP); Sb – stibnite,  $L\alpha$  (PETJ), Bi – synthetic Bi<sub>2</sub>Se<sub>3</sub>,  $M\alpha$  (PETH); S – sphalerite,  $K\alpha$  (PETJ); Se – naumannite,  $K\alpha$  (LIF). The CITZAF routine in the JEOL software, which is based on the  $\phi$ ( $\rho$ Z) method (Armstrong, 1995), was used for data processing.

Hansblockite displays only weak variations in composition (Tables 2, 3). In addition to the major cations Cu, Hg, Pb, Bi and Se, the only other omnipresent minor elements are Ag (0.4-1.3 wt.%); likely substituted for monovalent Cu) and Ni, with concentrations between <0.1 and 0.6 wt%. Trace amounts of Co (< 0.1 wt.%) were detected occasionally. Copper and Hg, and Bi and Pb are antipathetically correlated, which argues for operation of the coupled substitution  $Hg^{2+} + Pb^{2+} \leftrightarrow Cu^+ + Bi^{3+}$ . The mean empirical formula (based on 4 atoms pfu) of hansblockite is  $(Cu_{0.68}Hg_{0.27}Ag_{0.03}Ni_{0.01})_{\Sigma=0.99}(Bi_{0.69}Pb_{0.31})_{\Sigma=1.00}Se_{2.01}$  (n = 28). The ideal formula is  $(Cu,Hg)(Bi,Pb)Se_2$ . Table 3 presents a compilation of representative results of electron-

169	microprobe spot analyses of hansblockite and grundmannite, ideally CuBiSe <sub>2</sub> . Compositional
170	data for other Cu-(Pb)-(Hg)-Bi-Se minerals from El Dragón (petrovicite, watkinsonite,
171	eldragónite, unnamed phases "A" and "C") are reported in Förster et al., 2016, their Table 3).
172	The mean compositions of these phases, together with that of hansblockite, could be
173	displayed, for instance, in the Cu – (Hg+Ag) – Bi ternary diagram (Fig. 6), demonstrating that
174	hansblockite (previously phase "B") is chemically distinct from phases "A" and "C".
175	
176	Crystal structure
177	X-ray powder-diffraction data
178	The observed powder diffraction pattern (Table 4) of the same hansblockite fragment used for
179	the single-crystal study (see below) was collected with a CCD-equipped diffractometer
180	Xcalibur PX Ultra using $CuK\alpha$ radiation (50 kV and 40 mA – 5 hs as exposition time).
181	Crystal-to-detector distance was 7 cm. Data were processed using the CrysAlis software
182	package version 1.171.31.2 (Oxford diffraction, 2006) running on the Xcalibur PX control
183	PC. The unit-cell parameters obtained from powder data (pseudo-Gandolfi mode), using the
184	software <i>UnitCell</i> (Holland and Redfern, 1997), are: $a = 6.8529(4)$ Å, $b = 7.6388(5)$ Å, $c =$
185	7.2669(6) Å, $\beta$ 97.662(5)°, $V = 377.01(3)$ Å <sup>3</sup> , in excellent agreement with those obtained
186	from single-crystal data ( <i>cf.</i> , Table 5).
187	X-ray single-crystal data
188	A single hansblockite fragment (35 $\times$ 40 $\times$ 55 $\mu m) was mounted on a 0.005-mm-diameter$
189	carbon fiber and checked on a CCD-equipped Oxford Diffraction Xcalibur 3 single-crystal

diffractometer, operating with MoK $\alpha$  radiation ( $\lambda = 0.71073$  Å). The unit-cell values are: a =

6.853(1) Å, b = 7.635(1) Å, c = 7.264(1) Å,  $\beta = 97.68(1)^{\circ}$ , V = 376.66(9) Å<sup>3</sup>. It showed an

excellent diffraction quality and was used for full data collection (Table 5). Intensity

190

191

integration and standard Lorentz-polarization corrections were performed with the CrysAlis
RED (Oxford Diffraction, 2006) software package. The program ABSPACK of the CrysAlis
RED package (Oxford Diffraction, 2006) was used for the absorption correction. Reflection
conditions were consistent with space group $P2_1/c$ . The full-matrix least-squares program
SHELXL-97 (Sheldrick, 2008), working on $F^2$ , was used for the refinement of the structure.
Given the close stoichiometry and the similarity in the unit-cell values, refinement was done
starting from the atomic coordinates reported for synthetic copper chalcogenides with the
formula $LnCuQ_2$ (Ln = rare-earth element, Sc, Y; Q = S, Se, Te; Ijjaali et al., 2004). Site-
scattering values were refined using scattering curves for neutral species (Ibers and Hamilton,
1974) as follows: Cu vs. [] (structural vacancy) and Bi vs. [] for the cation sites, and Se vs. []
for the anion sites. The Se sites were found fully occupied, and the occupancy factors were
then fixed to 1.00. The electron density refined at the metal sites (43.8 and 82.7 for the Cu and
Bi site, respectively) is in excellent agreement with the electron-microprobe data (Tables 2,
3). Successive cycles were run introducing anisotropic temperature factors for all the atoms
leading to $R_1 = 0.0314$ for 713 observed reflections $[F_o > 4\sigma(F_o)]$ and $R_1 = 0.0345$ for all
1,627 independent reflections. Fractional atomic coordinates and isotropic atomic
displacement parameters are reported in Table 6 whereas the bond distances are given in
Table 7. Structure factors and CIF are deposited with the Principal Editor of Mineralogical
Magazine at http://www.minersoc.org/pages/e_iournals/dep_mat.html.

### **Results and Discussion**

## Crystal-chemical remarks

The crystal structure of hansblockite (Fig. 7) is topologically identical to that reported for several ternary rare-earth copper chalcogenides  $LnCuQ_2$  (Ln = rare-earth element, Sc, Y; Q = S, Se, Te). These compounds show interesting optical, magnetic, and thermoelectric

properties (e.g., Ijjaali *et al.*, 2004). In the structure, each (Bi,Pb) atom is surrounded by seven Se atoms [3Se(1) + 4Se(2)] to form a monocapped trigonal prism (Fig. 7). These prisms share edges and caps to form double layers that stack perpendicular to the **a**-axis. These double layers are separated by layers of (Cu,Hg) atoms, each atom being tetrahedrally coordinated by four Se atoms [3Se(1) + 1Se(2)]. Alternatively, the structure may be thought of as consisting of [Cu,Hg]Se<sub>2</sub> sheets separated by (Bi,Pb) atoms along the **a**-axis.

The mineral chemistry (*cf.*, Tables 2, 3) is in perfect agreement with the results of the structure refinement. The mean bond distance observed for the (Cu,Hg)-tetrahedron (2.536 Å) matches very well that calculated from the weighted bond distance 0.70(Cu–Se) + 0.30(Hg–Se) = 2.544 Å [using the ideal (pure) tetrahedral Cu–S and Hg–S distances in grundmannite (Förster *et al.*, 2016) and tiemannite (Wiegers, 1971), respectively]. The 7-fold coordinated (Bi,Pb) site shows a mean bond distance of 3.072 Å, in perfect agreement with the typical environments formed by these cations.

Noteworthy, the cation coordinations in hansblockite differ from those in the orthorhombic CuBiSe<sub>2</sub> polymorph grundmannite. In the latter, Bi forms BiSe<sub>3</sub> trigonal pyramids (with two additional longer distances), while Cu forms nearly regular CuSe<sub>4</sub> tetrahedra. The mean Cu–Se tetrahedral bond distance in grundmannite is 2.505 Å (Förster *et al.*, 2016), which compares favorably with that observed in hansblockite (2.536 Å).

Hansblockite represents the monoclinic polymorph of CuBiSe<sub>2</sub>, after the recently reported orthorhombic grundmannite (Förster *et al.*, 2016). We prefer to propose the hansblockite formula as  $(Cu,Hg)(Bi,Pb)Se_2$  (instead of CuBiSe<sub>2</sub>), because Hg and Pb seem fundamental to stabilize the monoclinic structure via the coupled substitution  $Hg^{2+} + Pb^{2+} \leftrightarrow Cu^+ + Bi^{3+}$ .

# Origin of hansblockite

Selenium and accompanying elements (Cu, Ag, Co, Ni, Pb, Hg, Bi,) were most likely
mobilized from a Kupferschiefer-type reduced black shale rich in framboidal pyrite, copper
sulfides, and organic material (Förster et al., 2016). The Se-mineralization was deposited in a
fault zone at the contact of that shale with a hematite-rich, oxidized siltstone. Transport and
deposition of Se and accompanying elements involved a low-T hydrothermal fluid and took
place during one single event. Hansblockite postdates the formation of the
krut'aite-penroseite solid-solution series that forms the bulk of the Se ore. Deposition of these
minerals resulted in enrichment of the ore-forming fluid in elements poorly compatible with
their structure, i.e., Hg, Pb and Bi. Hansblockite was deposited from this enriched fluid,
together with the bulk of the other Cu-Hg-Pb-Bi-Se minerals. It little predates the formation
of its orthorhombic polymorph, grundmannite, which is among the youngest primary Se-
minerals forming the El Dragón deposit (Förster et al., 2016). As for grundmannite,
hansblockite is cogenetic with klockmannite, umangite and clausthalite, simple selenides for
which the thermodynamic properties are well constrained (Simon and Essene, 1996). The
absence of berzelianite and bellidoite implies that the selenium fugacity was in a range from
below the krut'aite-klockmannite univariant reaction to above the umangite-berzelianite
univariant reaction [( $\log f \text{Se}_2 = -10.5 \text{ to } -14.5 \text{ for } T = 100 ^{\circ}\text{C}$ ( <i>cf.</i> , Simon and Essene, 1997)].
The presence of hematite/goethite and the absence of chalcopyrite, pyrite and bornite suggest
$log f S_2 < -17$ . Thus, hansblockite precipitated at a $f Se_2/f S_2$ ratio $> 1$ , as typifying the
environment of formation of telethermal vein-type selenide mineralization (Simon and
Essene, 1997).

# Acknowledgements

266	Dieter Rhede (formerly Deutsches GeoForschungsZentrum GFZ, Potsdam, Germany) is
267	thanked for his assistance with the electron-microprobe work. CJS acknowledges Natural
268	Environment Research Council grant NE/M010848/1 Tellurium and Selenium Cycling and
269	Supply. The research was partially supported by "progetto d'Ateneo 2013. Università di
270	Firenze" to LB.
271	
272	References
273	Armstrong, J.T. (1995) CITZAF: a package of correction programs for the quantitative electron
274	microbeam X-ray-analysis of thick polished materials, thin films, and particles. Microbeam
275	Analysis, 4, 177–200.
276	Bannister, F.A. and Hey, M.H. (1937) The identity of penroseite and blockite. American Mineralogist,
277	<b>22</b> , 319–324.
278	Block, H. (1937) Das Selenvorkommen von Pacajake in Bolivien. Erzmetall, 34, 237–238.
279	Block, H. and Ahlfeld, F. (1937) Die Selenlagerstätte Pacajake, Bolivia. Zeitschrift für praktische
280	<i>Geologie.</i> , <b>45</b> , 9–14.
281	Förster, HJ., Bindi, L. and Stanley, C.J. (2016) Grundmannite, CuBiSe <sub>2</sub> , the Se-analogue of
282	emplectite: a new mineral from the El Dragón mine, Potosí, Bolivia. European Journal of
283	Mineralogy, doi: 10.1127/ejm/2016/0028-2513.
284	Grundmann, G., Lehrberger, G. and Schnorrer-Köhler, G. (1990) The El Dragón mine, Potosí, Bolivia.
285	Mineralogical Record, 21, 133–146.
286	Herzenberg, R. and Ahlfeld, F. (1935) Blockit, ein neues Selenerz aus Bolivien. Zentralblatt für
287	Mineralogie, Geologie und Paläontologie (Abteilung A), <b>9</b> , 277–279.
288	Holland, T.J.B. and Redfern, S.A.T. (1997) UNITCELL: a nonlinear least-squares program for cell-
289	parameter refinement and implementing regression and deletion diagnostics. Journal of
290	Applied Crystallography, <b>30</b> , 84–84.

291	Ibers, J.A. and Hamilton, W.C. Eds. (1974) International Tables for X-ray Crystallography, vol. IV,
292	366p. Kynock, Dordrecht, The Netherlands. LnCuSe <sub>2</sub> (Ln = La, Ce, Pr, Nd, Sm).
293	Ijjaali, I., Mitchell, K. and Ibers, J.A. (2004) Preparation and structure of the light rare-earth copper
294	selenides <i>Ln</i> CuSe <sub>2</sub> ( <i>Ln</i> = La, Ce, Pr, Nd, Sm). <i>Journal of Solid State Chemistry</i> , <b>177</b> , 760–764.
295	Kampf, A.R., Mills, S.J., Nash, B.P., Thorne, B. and Favreau, G. (2016) Alfredopetrovicite: a new
296	selenite mineral from the El Dragón mine. European Journal of Mineralogy, doi:
297	10.1127/ejm/2015/0027-2506
298	Mills, S. J., Kampf, A.R., Christy, A.G., Housley, R. M., Thorne, B., Chen, Yu-Sheng and Steele, I. M.
299	(2014) Favreauite, a new selenite mineral from the El Dragón mine, Bolivia. European
300	Journal of Mineralogy, <b>26</b> , 771–781.
301	Oxford Diffraction (2006) CrysAlis RED (Version 1.171.31.2) and ABSPACK in CrysAlis RED.
302	Oxford Diffraction Ltd, Abingdon, Oxfordshire, England.
303	Paar, W.H., Cooper, M.A., Moëlo, Y., Stanley, C.J., Putz, H., Topa, D., Roberts, A.C., Stirling, J.,
304	Raith, J.G. and Rowe, R. (2012) Eldragónite, Cu <sub>6</sub> BiSe <sub>4</sub> (Se) <sub>2</sub> , a new mineral species from the
305	El Dragón mine, Potosí, Bolivia, and its crystal structure. Canadian Mineralogist, 50,
306	281–294.
307	Sheldrick, G.M. (2008) A short history of SHELX. Acta Crystallografica, A64, 112–122.
308	Simon, G. and Essene, E.J. (1996) Phase relations among selenides, sulphides, tellurides, and oxides:
309	I. Thermodynamic properties and calculated equilibria. <i>Economic Geology</i> , <b>91</b> , 1183–1208.
310	Simon, G. and Essene, E.J. (1997) Phase relations among selenides, sulphides, tellurides, and oxides:
311	II: Applications to selenide-bearing ore deposits. <i>Economic Geology</i> , <b>92</b> , 468–484.
312	Wiegers, G.A. (1971) The crystal structure of the low-temperature form of silver selenide. <i>American</i>
313	Mineralogist, <b>56</b> , 1882–1888.
314	
315	
316	

### Figure captions

317

318 FIG. 1. Back-scattered electron (BSE) image, demonstrating the angular network-like intersetal texture 319 typical for hansblockite-bearing mineral aggregates. Lath-shaped thin plates of hansblockite (light 320 gray) overgrowing elongated plates of unnamed phase "A" selenide (dark gray), which predate 321 hansblockite and were deposited in the core. The bright mineral represents clausthalite. 322 FIG. 2. Reflected light (top) and BSE (bottom) images of hansblockite (hb) in association with 323 clausthalite (cl), krut'aite—penroseite solid solution (k-p), eskebornite (esk), klockmannite (kl), 324 eldragónite (eld), and petrovicite (pet). Horizontal field of view is ~200 μm. The crystal used for 325 structural analysis was separated from this area. 326 FIG. 3: Reflected light images (200 µm width each) of hansblockite and associated minerals. Right 327 hand side with partly crossed polarizers, left hand side without. Top and bottom row correspond to different extinction rotations. hb = hansblockite, "A" = phase "A", pet = petrovicite, cl = clausthalite, u 328 329 = umangite, kl = klockmannite, k-p = krut'aite-penroseite solid solution. In plane-polarized incident 330 light, hansblockite is cream to light grey in colour, slightly bireflectant and slightly pleochroic from 331 greyish cream to cream. The mineral does not show any internal reflections. Under crossed polars, 332 hansblockite is weakly anisotropic with khaki to pale blue rotation tints. 333 FIG. 4. Reflected light images (200 um width each) of hansblockite and associated minerals. Right 334 hand side with partly crossed polarizers, left hand side without. Top and bottom row correspond to 335 different extinction rotations. See Fig. 3 for abbreviations of mineral names. Note the overgrowth of 336 hansblockite on phase "A" nicely demonstrated in the right hand side-image of the bottom row. 337 FIG. 5. Reflectance spectra of hansblockite and its orthorhombic dimorph grundmannite (Förster et al., 338 2016). 339 FIG. 6. Cu – (Hg+Ag) – Bi (apfu) ternary diagram showing the mean composition of minerals of the 340 Cu-Hg-Pb-Bi-Se system from El Dragón. Data sources: Förster et al. (2016); this work.

FIG. 7. The crystal structure of hansblockite projected down [010]. The horizontal direction is the *c*-axis. (Cu,Hg) atoms are depicted as light-blue tetrahedral, whereas (Bi,Pb) and Se are given as blue and small red spheres, respectively. The coordination of the (Bi,Pb) atom is shown on the right.

341

342

Table 1. Reflectance data and colour values for hansblockite.

λ (nm)	$R_1(\%)$	R <sub>2</sub> (%)	λ (nm)	$R_1(\%)$	$\mathbf{R}_{2}$ (%)
400	46.7	46.9	640	46.7	48.6
420	46.9	47.1	660	46.5	48.4
440	47.1	47.4	680	46.4	48.2
460	47.3	47.9	700	46.3	48.0
480	47.4	48.4			
500	47.4	48.7	Commis	sion on Ore M	ineralogy
520	47.4	48.9		wavelengths	
540	47.4	49.0			
560	47.3	49.0	470	47.3	48.1
580	47.2	49.0	546	47.4	49.0
600	47.0	48.9	589	47.1	49.0
620	46.9	48.8	650	46.6	48.5

## **Colour values**

	C illu	minant	A illu	minant
	$R_1$ $R_2$		$R_1$	$R_2$
X	0.310	0.312	0.447	0.448
y	0.317	0.320	0.408	0.409
Y (%)	47.2	48.9	47.2	48.9
$\Delta_{ m d}$	519	568	511	577
P <sub>e</sub> (%)	0.2	1.5	0.2	1.8

Table 2. Composition of hansblockite (wt.%) from El Dragón.

	Cu	Ag	Hg	Pb	Co	Ni	Bi	Se	Total
mean	9.31	0.73	11.43	13.55	0.03	0.17	31.17	34.00	100.39
1σ	0.43	0.25	0.30	0.24	0.03	0.14	0.26	0.32	0.46
min	8.14	0.42	11.00	13.04	0.00	0.03	30.76	33.53	99.40
max	10.01	1.29	12.23	14.23	0.07	0.65	31.77	34.76	101.77

*Notes:*  $1\sigma = 1\sigma$  standard deviation.

Table 3. Representative results of electron-microprobe spot analyses of hansblockite and grundmannite from El Dragón.

mineral				hansblockit	te			٤	grundmann	ite	
element	d.l. (ppm)	1	2	3	4	5	6	7	8	9	10
Cu (wt.%)	250	8.95	9.80	9.37	9.63	8.52	14.88	14.96	14.78	15.01	14.82
Ag	200	1.29	0.45	0.43	0.49	1.07	0	0	0	0	0
Hg	1100	11.55	11.15	12.23	11.41	11.60	0.24	0	0	0.11	0
Pb	400	13.78	13.35	13.54	13.66	14.23	1.32	1.14	0.99	1.22	1.20
Fe	200	0	0	0	0	0	0	0	0	0	0
Zn	200	0	0	0	0	0	0	0	0	0	0
Co	200	0.06	0.07	0	0	0.04	0	0	0	0	0
Ni	200	0.40	0.65	0.09	0.08	0.05	0	0.18	0	0.22	0.05
As	250	0	0	0	0	0	0	0	0	0	0
Sb	300	0	0	0	0	0	0	0	0	0	0
Bi	300	30.71	30.99	31.12	31.25	30.74	44.71	44.81	45.13	44.65	44.86
S	150	0	0	0	0	0	0	0	0	0	0
Se	800	33.99	33.87	33.52	33.85	33.55	38.77	39.33	38.84	38.78	38.66
total		100.72	100.34	100.28	100.35	99.79	99.92	100.41	99.74	99.99	99.59
Cu (apfu)		0.65	0.71	0.69	0.71	0.64	0.99	0.98	0.98	0.99	0.99
Ag		0.06	0.02	0.02	0.02	0.05					
Hg		0.27	0.26	0.29	0.27	0.27	0.01				
Pb		0.31	0.30	0.31	0.31	0.33	0.03	0.02	0.02	0.02	0.02
Co			0.01								
Ni		0.03	0.05	0.01	0.01			0.01		0.02	0.00
Bi		0.68	0.68	0.70	0.70	0.70	0.90	0.90	0.91	0.90	0.91
Se		2.00	1.98	1.99	2.00	2.01	2.07	2.08	2.08	2.07	2.07

d.l.: detection limit. 0: sought, but not detected. Formula proportions were calculated on the basis of 3 apfu.

Table 4. Measured and calculated X-ray powder diffraction data (d in Å) for hansblockite.

hkl	$d_{meas}$	$I_{ m obs}$	$d_{calc}$	$I_{ m calc}$
-111	4.37	20	4.3575	22
111	3.97	90	3.9653	90
002	-	-	3.5994	6
021	-	-	3.3726	8
-102	3.375	10	3.3723	15
-121	3.100	40	3.0990	43
-112	-	-	3.0848	7
102	-	-	3.0179	10
-211	2.986	100	2.9849	100
112	2.808	50	2.8066	58
211	2.732	10	2.7307	14
-202	-	-	2.6534	9
022	2.620	60	2.6189	64
220	2.534	25	2.5372	28
-122	2.525	20	2.5274	17
-221	2.470	10	2.4716	13
031	2.400	20	2.3995	19
130	2.385	30	2.3832	36
202	2.321	20	2.3201	18
-131	2.296	25	2.2948	22
013	2.290	35	2.2892	32
300	_	_	2.2638	11
131	_	_	2.2314	5
310	2.171	10	2.1704	11
-311	_	_	2.1558	8
113	_	_	2.0901	6
230	_	_	2.0365	6
-213	2.022	5	2.0214	12
-123	2.010	20	2.0098	22
311	2.008	10	2.0082	16
222	-	-	1.9827	6
-312	1.974	10	1.9739	15
320	_	_	1.9472	6
132	1.946	10	1.9455	12
140	1.839	5	1.8376	12
321	1.828	15	1.8275	16
-322	1.802	15	1.8015	12
004	-	-	1.7997	8
312	_	_	1.7615	6
-204	1.687	10	1.6862	9
223	-	-	1.6625	7
-233	1.618	5	1.6180	9
-233	1.010	3	1.0100	9

241	1.600	5	1.5984	9
124	-	-	1.5414	7
313	-	-	1.5159	6
-304	-	-	1.5105	6
-341	1.455	10	1.4548	12
015	-	-	1.4148	6
-432	-	-	1.3675	7
-252	-	-	1.3235	8
-334	-	-	1.2990	5
450	-	-	1.1354	5

*Note* = calculated diffraction pattern obtained with the atom coordinates reported in Table 6 (only reflections with  $I_{\text{rel}} \ge 5$  are listed).

Table 5. Data and experimental details for the selected hansblockite crystal.

### Crystal data

Formula (Cu,Hg)(Bi,Pb)Se<sub>2</sub>  $0.035 \times 0.040 \times 0.055$ Crystal size (mm) Form block Colour black Crystal system monoclinic Space group  $P2_1/c$ a (Å) 6.853(1) b (Å) 7.635(1)c (Å) 7.264(1)β (°) 97.68(1) V (Å<sup>3</sup>) 376.66(9) Z

#### **Data collection**

Instrument Oxford Diffraction Xcalibur 3 Radiation type  $MoK\alpha (\lambda = 0.71073 \text{ Å})$ Temperature (K) 293(2) Detector to sample distance (cm) 5 Number of frames 482 Measuring time (s) 80 Maximum covered 2θ (°) 70.00 Absorption correction multi-scan (ABSPACK; Oxford Diffraction, 2006) Collected reflections 6599 Unique reflections 1627 713

Unique reflections 1627
Reflections with  $F_o > 4\sigma(F_o)$  713  $R_{int}$  0.0308  $R_{\sigma}$  0.0431

Range of h, k, l  $-11 \le h \le 11, -12 \le k \le 12, -11 \le l \le 11$ 

### Refinement

Refinement Full-matrix least squares on  $F^2$ 

Final  $R_1$  [ $F_0 > 4 \sigma$  ( $F_0$ )] 0.0314 Final  $R_1$  (all data) 0.0345 Number of least squares parameters 39 Goodness of Fit 0.934

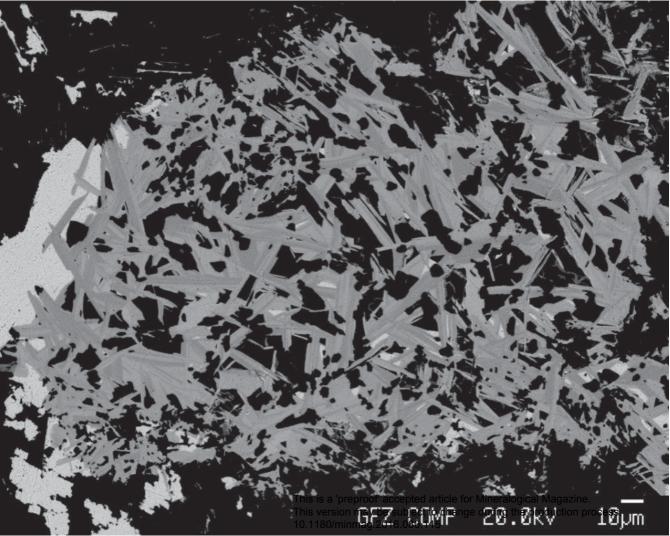
 $\Delta \rho_{\text{max}}$  (e Å<sup>-3</sup>) 1.27 (2.11 Å from Bi)  $\Delta \rho_{\text{min}}$  (e Å<sup>-3</sup>) -1.33 (0.73 Å from Se2)

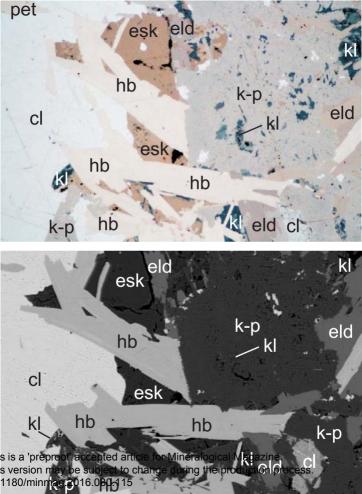
Table 6. Atom coordinates and equivalent isotropic displacement parameters  $(\mathring{A}^2)$  for hansblockite.

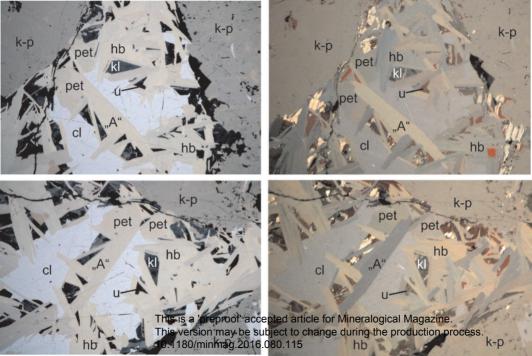
atom	Site occupancy	x/a	y/b	z/c	$U_{ m iso}*/U_{ m eq}$
(Cu,Hg)	$Cu_{0.71}Hg_{0.29}$	0.0709(2)	0.6630(2)	0.0531(2)	0.0154(4)
(Bi,Pb)	$Bi_{0.70}Pb_{0.30}$	0.3087(1)	0.05019(9)	0.20049(9)	0.0192(2)
Se1	$Se_{1.00}$	0.0951(3)	0.3895(3)	0.2764(3)	0.0228(5)
Se2	$Se_{1.00}$	0.5869(3)	0.2728(3)	0.0010(3)	0.0215(5)

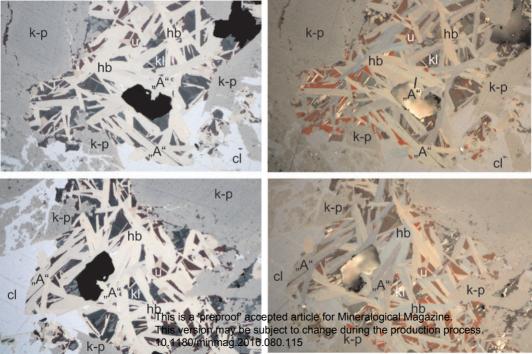
Table 7. Selected bond distances (Å) for hansblockite.

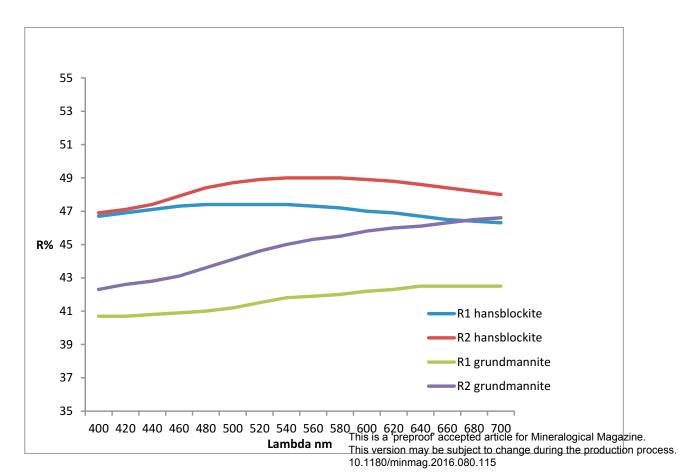
Cu-Se2	2.478(3)	Bi-Se2 3.019(2)	Bi-Cu 3.458(2)
Cu-Se1	2.489(2)	Bi-Se1 3.047(2)	Bi-Cu 3.475(2)
Cu-Se1	2.541(3)	Bi-Se1 3.052(2)	
Cu-Se1	2.636(2)	Bi-Se2 3.060(2)	
Cu-Cu	2.745(3)	Bi-Se1 3.062(2)	
		Bi-Se1 3.262(2)	

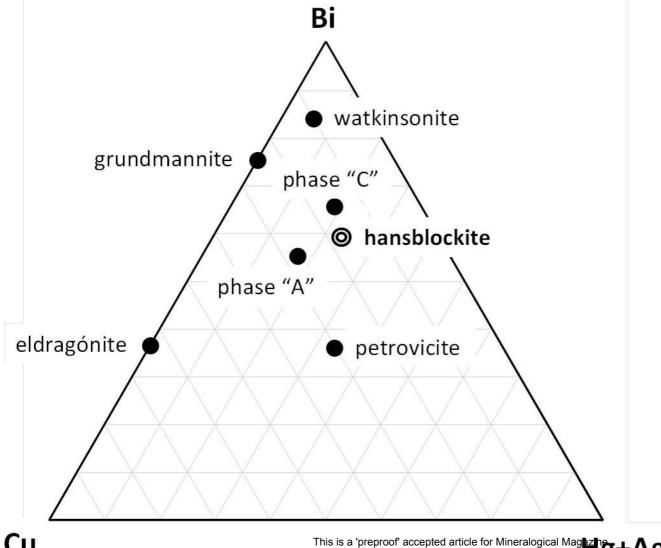












Cu

This is a 'preproof' accepted article for Mineralogical Magazine This version may be subject to change during the product of 10.1180/minmag.2016.080.115

